

Delocalization and hybridization enhance the magnetocaloric effect in $\text{Ni}_2\text{Mn}_{0.75}\text{Cu}_{0.25}\text{Ga}$

S Roy^{1,*}, E. Blackburn^{2,‡}, S. M. Valvidares³, M. R. Fitzsimmons⁴, Sven C. Vogel⁴, M. Khan⁵, I. Dubenko⁵, S. Stadler⁵, N. Ali⁵, S. K. Sinha² and J. B. Kortright³

¹ Advanced Light Source, Lawrence Berkeley National Laboratory, Berkeley, California 94720, USA.

² Department of Physics, University of California San Diego, La Jolla, California 92093, USA.

³ Materials Sciences Division, Lawrence Berkeley National Laboratory, Berkeley, California 94720, USA

⁴ Manuel Lujan Neutron Scattering Center, Los Alamos National Laboratory, Los Alamos, New Mexico 87545, USA

⁵ Department of Physics, Southern Illinois University, Carbondale, Illinois 62901, USA

[‡] Present address: School of Physics and Astronomy, University of Birmingham, Birmingham, B15 2TT, UK.

* Corresponding author: sroy@lbl.gov

In view of the looming energy crisis facing our planet, attention increasingly focuses on materials potentially useful as a basis for energy saving technologies. The discovery of giant magnetocaloric (GMC) compounds - materials that exhibit especially large changes in temperature as the externally applied magnetic field is varied - is one such compound ¹. These materials have potential for use in solid state cooling technology as a viable alternative to existing gas based refrigeration technologies that use chloro-fluoro - and hydro-fluoro-carbon chemicals known to have a severe detrimental effect on human health and environment ^{2,3}. Examples of GMC compounds include $Gd_5(SiGe)_4$ ⁴, $MnFeP_{1-x}As_x$ ⁵ and Ni-Mn-Ga shape memory alloy based compounds ⁶⁻⁸. Here we explain how the properties of one of these compounds (Ni_2MnGa) can be tuned as a function of temperature by adding dopants. By altering the free energy such that the structural and magnetic transitions coincide, a GMC compound that operates at just the right temperature for human requirements can be obtained ⁹. We show how Cu, substituted for Mn, pulls the magnetic transition downwards in temperature and also, counterintuitively, increases the delocalization of the Mn magnetism. At the same time, this reinforces the Ni-Ga chemical bond, raising the temperature of the martensite-austenite transition. At 25% doping, the two transitions coincide at 317 K.

Ni-Mn-Ga based alloy is a multifunctional material that exhibits several interesting properties ^{7,10,11} - the magnetocaloric effect being one of them. One key property of these alloys is the existence of an austenite (high temperature) to martensite (low temperature) first order structural phase transition and a second order magnetic

phase transition. In Ni_2MnGa , these two transition temperatures are 225 and 384 K respectively¹². Each of these phase transitions has an associated, weak magnetocaloric effect.

It has been found that if the structural and magnetic transitions can be tuned to occur at the same temperature, the entropy change (a measure of the magnetocaloric effect) of the joint transition is significantly enhanced compared to that of the separated transitions, leading to the GMC effect. For example, by increasing the Ni content, entropy changes in the range -3.5 to -20.4 J/Kg K have been obtained in polycrystals, while in single crystals the change observed has been as high as -86 J/kg K⁶⁻⁸. The transitions can also be tuned by atomic substitution at the Mn or at the Ga sites^{12,13}. In particular, 25% Cu at the Mn site results in a ΔS of ~ -60 J/kg K in the temperature range 308 - 334 K^{9,14}. $\text{Ni}_2\text{Mn}_{0.75}\text{Cu}_{0.25}\text{Ga}$ is thus promising as a magnetic refrigerant. But the physics underlying the enhancement of GMC properties of this system has not been convincingly understood.

Ferromagnetism in the Ni_2MnGa family of compounds is localized, and is primarily due to indirect RKKY interactions between neighboring Mn atoms, mediated by conduction electrons^{15,16}. The minority spin electrons in the d band of the Mn are almost excluded from the conduction band, and hence give rise to a localized magnetic moment. Since the magnetic and structural properties are intricately linked by the lattice parameter ratio c/a ¹⁷⁻²⁰ as well as the density of 3d electrons at the Fermi level^{20,21}, replacement of Mn by Cu should cause site - and element - specific changes in the electronic and magnetic properties. A detailed understanding of such changes is essential

for further development and improvement of these materials, and the motivation for this study.

We have performed systematic X-ray absorption spectroscopy (XAS), magnetic circular dichroism (XMCD) studies at the $L_{2,3}$ edges of the constituent elements of Ni_2MnGa and the substituted compound $\text{Ni}_2\text{Mn}_{0.75}\text{Cu}_{0.25}\text{Ga}$ as a function of temperature to directly probe the d electrons and their respective contribution to the electronic and magnetic properties. Magnetization and the nature of the phase transition have been determined by magnetometry and neutron diffraction studies. We find that Cu substitution has two fold effects. One, it increases the covalent character of Ni that results in an enhanced Ni-Ga hybridization thereby affecting the martensitic transition temperature. Second, due to Cu substitution, the Mn content is reduced that weakens the magnetic ordering temperature. Another interesting effect is that it enhances the delocalization of the magnetism from Mn. The combined XAS, XMCD, neutron and magnetometry results lead to a coherent, atomic-scale understanding of how changes in the electronic properties lead to the enhanced thermodynamic properties of the giant magnetocaloric effect in $\text{Ni}_2\text{Mn}_{0.75}\text{Cu}_{0.25}\text{Ga}$.

Fig. 1(a) shows the magnetization versus temperature curves from 75 – 400 K for Ni_2MnGa and $\text{Ni}_2\text{Mn}_{0.75}\text{Cu}_{0.25}\text{Ga}$ taken at 1 kOe. Ni_2MnGa shows a second order paramagnetic to ferromagnetic phase transition at 386 K (T_C) and a first order change in magnetization at 208 K (T_M) associated with martensitic structural transition. On substituting Mn by Cu the second order magnetic and first order structural transition temperature move in opposite directions, and for 25% Cu merge into a single first order phase transition at 317 K (Fig 1(a))⁹. This merging of T_C and T_M however comes at the

cost of overall reduction of magnetization in $\text{Ni}_2\text{Mn}_{0.75}\text{Cu}_{0.25}\text{Ga}$ as compared to Ni_2MnGa . This reduction is $\sim 25\%$ (see Fig 1(a)) and correlates with the decreased Mn concentration. The nature of the phase transition has been further confirmed by temperature dependent neutron diffraction (Fig 1(b)). The single (002) peak above the transition temperature splits due to the cubic-to-tetragonal structural transition. The presence of three clear peaks around the phase transition temperature ($307 \text{ K} \leq T \leq 305 \text{ K}$) shows that the cubic austenitic and tetragonal martensitic phases coexist close to the transition. This confirms the first order nature of the magneto-structural transition in $\text{Ni}_2\text{Mn}_{0.75}\text{Cu}_{0.25}\text{Ga}$.

To understand the underlying physics, we first determine the changes in electronic and magnetic structure in $\text{Ni}_2\text{Mn}_{0.75}\text{Cu}_{0.25}\text{Ga}$ due to the phase transition, and then compare the properties of $\text{Ni}_2\text{Mn}_{0.75}\text{Cu}_{0.25}\text{Ga}$ with the parent compound Ni_2MnGa . Changes to the electronic structure of the constituent elements of $\text{Ni}_2\text{Mn}_{0.75}\text{Cu}_{0.25}\text{Ga}$ were determined from XAS measured at 80 and 300 K (Fig 2(a-d)). The multiplet structure evident at the Ni and Mn L_{23} edges, in these metallic samples, is taken to result from partial localization of the electronic structure around the core-excited species and from hybridization effects reflecting the ground-state band structure. For Ni, these structures at the L_3 are the features marked A and B, and, although weak, are clearly present at the L_2 edge (feature C). There is no significant change in A over the entire temperature range measured while feature B weakens and shifts upwards in energy on lowering the temperature (by 1.5 eV at 80 K relative to 300 K – see Fig. 2a inset). This feature B, which is 5 eV above the main L_3 peak, represents the Ni $2p3d^{10}$ state that hybridizes with Ga p states²². Extending this interpretation, we thus interpret the broadening of the

feature B due to the martensitic transition as evidence of increase in the covalent character of Ni resulting from increased hybridization with Ga. A similar shift is also observed for feature C (Fig. 2(a)).

The Mn XAS (Fig. 2(b)) also shows multiplet structure (features D, E and F) characteristic of primarily d^5 with some d^6 ground states. Although there are discussions about selective oxidation in the literature as the reason for the multiplet features in the Mn, a multitude of experimental results reported on similar compounds increasingly suggest rather a modification of the band structure being responsible for the observed line shapes²²⁻²⁵. This is consistent with band structure calculations^{16,20,26}, and the observation of Jahn-Teller effect in these compounds which lifts the d orbital degeneracy and effectively narrows the band²⁷. A weak bump (feature F) is observed 5 eV above the main peak (637.4 eV) at 642.8 eV (inset Fig. 2(b)). The feature is absent for Ni₂MnGa at 80 K. Since density of state (DOS) calculations show that there are no Mn-Ga hybridized states in Ni₂MnGa and Ni rich Ni₂MnGa while Ni-Mn hybridized states are available^{20,26}, we ascribe the bump in the Mn spectrum to a weak Mn d -Ni d interaction. Integrated intensity under the curve by Gaussian fit reveals that the peak is stronger at 330 K by ~ 8.5% than at 80 K with no change in the peak position as a function of energy. Thus the magneto-structural transition results in a redistribution of the d electrons with negligible change in the d - d interaction energy. The redistribution of electron is consistent with our observation of increased intensity at low temperature. In particular, it is likely that some of the Ni d electrons delocalize in the process, and some or all of these electrons may bond covalently with Ga p states. Indeed the XMCD data suggests this. Cu and Ga XAS show no discernible change as a function of temperature.

XMCD spectra taken at 80, 300 and 330 K are shown in Fig 2(e-h). Both Ni and Mn XMCD show multiplet structure at the $L_{2,3}$ edges consistent with published results^{22,23,28}. In the ferromagnetically ordered state Mn atomic moment increases by 61% at 80 K relative to 300 K. In comparison, the Ni moment only changes by 33%. The smaller change in the Ni moment relative to Mn is attributed to minority spin antibonding states above E_F which are primarily due to Mn while both the e_g states of Ni are below E_F ²⁰.

Significant XMCD was detected at the Ga L_3 and it follows the same temperature dependence as the Ni (Mn) magnetization by disappearing above T_C . The Ga XMCD signal is opposite to that of Ni and Mn which means that Ga induced spins are antiparallel to Ni and Mn spins, and in accord with published results^{16,27}. Recalling our earlier result from Fig 2(a) that for $T < T_M$ (T_C) the covalent character of Ni increases, the magnetic moment in Ga is then due to hybridization effects between the d states of Ni with Ga p states and does not come from direct exchange interaction. It is interesting to note that similar hybridization effects between Gd and Ge are also found in $Gd_5(SiGe)_4$ compounds²⁹. We did not observe any magnetic moment for Cu.

The effect of Cu substitution on the electronic structure in Ni and Mn is obtained from XAS measured at 80 K (Fig 3(a, b)). As shown in Fig 3(a), the $Ni_2Mn_{0.75}Cu_{0.25}Ga$ curve is slightly broader at both edges, implying a more dispersive, delocalized band structure. The most significant change on Cu substitution is seen at the feature B, which is the same feature of Fig 2(a). This feature is a distinct bump for Ni_2MnGa , whereas it is smeared out for $Ni_2Mn_{0.75}Cu_{0.25}Ga$. Mn XAS does not show a qualitative change in the spectral shape (Fig. 3(b)). It is noteworthy that both Ni and Mn XAS has higher intensity for $Ni_2Mn_{0.75}Cu_{0.25}Ga$ than Ni_2MnGa which could imply that there are fewer filled d

states immediately around Ni and Mn in $\text{Ni}_2\text{Mn}_{0.75}\text{Cu}_{0.25}\text{Ga}$ than in Ni_2MnGa , which is indicative of "ground-state" transfer of charge away from Ni and Mn. In the context of a slightly higher electronegativity of Cu than Mn or Ni, it is likely that Cu wants to completely fill its *s* and *d* shells by taking away charge from Ni and Mn when it is substituted. This "inertness" also explains absence of XMCD and negligible changes in Cu XAS.

Comparisons of element specific magnetic properties between Ni_2MnGa and $\text{Ni}_2\text{Mn}_{0.75}\text{Cu}_{0.25}\text{Ga}$ at 80 K are shown in Fig. 4. The XMCD signal of $\text{Ni}_2\text{Mn}_{0.75}\text{Cu}_{0.25}\text{Ga}$ is less than that of Ni_2MnGa , consistent with SQUID magnetometry (Fig. 1(a)). The Mn XMCD spectrum for $\text{Ni}_2\text{Mn}_{0.75}\text{Cu}_{0.25}\text{Ga}$ has a less pronounced multiplet structure indicating the increasingly delocalized character of the Mn *d* electrons. A clearer difference is observed for the Ni XMCD spectrum. The distinct shoulder A observed for Ni_2MnGa is broadened and feature B is weakened (Fig. 4(a)). The smearing out aspect of the multiplets observed in the XAS and XMCD results clearly shows that in $\text{Ni}_2\text{Mn}_{0.75}\text{Cu}_{0.25}\text{Ga}$, the Ni has a more covalent character, larger band spreading and hence more delocalized *d* electrons than Ni_2MnGa . A direct consequence of this is a higher level of hybridization between Ni *d* and Ga *p* bands which is also evidenced by the Ga XMCD results (Fig. 4(c)).

The above results show that a complex interplay between electronic, lattice and magnetic degrees of freedom determines the decrease (increase) of T_C (T_m) in Cu substituted Ni_2MnGa compounds. The hybridization and delocalization was found to be affected both by martensitic transition as well as Cu substitution. In particular, we find that by substituting 25% of Mn by Cu in Ni_2MnGa , the ferromagnetic austenitic phase is

suppressed and a single paramagnetic-austenitic to ferromagnetic-martensitic phase transition takes place at 317 K. This transition is first order in nature and this point to the fact that the magnetic transition in $\text{Ni}_2\text{Mn}_{0.75}\text{Cu}_{0.25}\text{Ga}$ is induced by the structural transition. In general, the magnetic interactions are weakened by Cu thereby reducing T_c , and make magnetism less localized from Mn. We also observe that in spite of the substitution being at the Mn site, significant changes happen at the Ni site. Cu substitution results in an enhancement of Ni covalency, and therefore a stronger Ni-Ga chemical bond. Since the martensitic transition is related to the formation of Ni d and Ga p hybrid states^{17,21}, a higher degree of Ni-Ga hybridization in $\text{Ni}_2\text{Mn}_{0.75}\text{Cu}_{0.25}\text{Ga}$ makes the chemical bond stronger so that more energy is required to trigger the martensitic transition. Addition of Cu therefore increases T_m at the same time as reducing T_c , and at 25% Cu substitution T_c and T_m coincide near room temperature, giving rise to the giant magnetocaloric effect.

Methods:

Polycrystalline stoichiometric Ni_2MnGa and $\text{Ni}_2\text{Mn}_{0.75}\text{Cu}_{0.25}\text{Ga}$ ingots were made from high purity elemental Ni, Mn, Cu and Ga using the conventional arc melting technique. Details of sample preparation can be found elsewhere^{9,12-14}. The phase purity of the samples was checked by X-ray diffraction using Cu K_α radiation at room temperature. Magnetization measurements were carried out by a SQUID magnetometer (Quantum Design, Inc.). Neutron diffraction was carried out on powdered samples at the Asterix (polarized neutron) and HIPPO (unpolarized neutron) beamlines of the Manuel Lujan Neutron Scattering Center, Los Alamos National Laboratory. X-ray absorption

spectroscopy (XAS) and X-ray Magnetic Circular Dichroism (XMCD) spectra were measured at the beamline 4.0.2 of the Advanced Light Source, Lawrence Berkeley National Laboratory. A small slice of the sample was cut from the bulk immediately prior to measurement to avoid surface contamination. Circularly polarized x-rays tuned to the $L_{2,3}$ edge of Ni, Mn, Cu and Ga were incident normal to the sample surface. The absorption was measured by total electron yield method.

Acknowledgements:

This work at ALS/LBNL was supported by the Director, Office of Science, Office of Basic Energy Sciences, of the U.S. Department of Energy under Contract No. DE-AC02-05CH11231. This work has benefited from the use of the Lujan Neutron Scattering Center at LANSCE, which is funded by the U.S. Department of Energy's Office of Basic Energy Sciences. Los Alamos National Laboratory is operated by Los Alamos National Security LLC under DOE contract DE-AC52-06NA25396. Work at UCSD was supported by the U.S. DOE/BES through contract No. DE/FG01-04ER04-01. Work at SIUC was supported by Research Corporation (RA0357), and by the U.S. DOE/BES through contract No. DE-FG02-06ER46291).

Competing Financial Interests: The authors declare no competing financial interests

References:

- [1]. Pecharsky, V. K. & Gschneidner Jr., K. A., Magnetocaloric effect and magnetic refrigeration. *J. Mag. Mag. Mater* **200**, 44 (1999).
- [2]. <http://www.epa.gov> ; <http://www.arap.org/index.html>
- [3] Recent estimates in the US put the share of hydro-fluoro-carbons to be about 0.8% in global warming. It is projected to increase to 2.3% by the year 2030 (<http://www.arap.org/adlittle/summary.html#2>) .
- [4]. Pecharsky, V. K. & Gschneidner Jr., K. A., Giant Magnetocaloric Effect in $\text{Gd}_5(\text{Si}_2\text{Ge}_2)$. *Phys. Rev. Lett.* **78**, 4494 (1997).
- [5]. Tegus, O., Brück, E. K., Buschow, H. J. & de Boer, F. R., Transition-metal-based magnetic refrigerants for room-temperature applications. *Nature* **415**, 150 (2002).
- [6]. Pareti, L., Solzi, M., Albertini, F. & Paoluzi, A., Giant entropy change at the co-occurrence of structural and magnetic transitions in the $\text{Ni}_{2.19}\text{Mn}_{0.81}\text{Ga}$ Heusler alloy. *Eur. Phys. J. B* **32**, 303 (2003).
- [7]. Zhou, X., Li, W., Kunkel, H. P. & Williams, G., A criterion for enhancing the giant magnetocaloric effect: (Ni–Mn–Ga)—a promising new system for magnetic refrigeration. *J. Phys: Condens Matter* **16**, L39 (2004).
- [8]. Pasquale, M., Sasso, C. P., Lewis, L. H., Giudici, L., Lograsso, T. & Schlagel, D., Magnetostructural transition and magnetocaloric effect in $\text{Ni}_{55}\text{Mn}_{20}\text{Ga}_{25}$ single crystals. *Phys Rev B* **72**, 094435 (2005).
- [9]. Stadler, S. *et al*, Magnetocaloric properties of $\text{Ni}_2\text{Mn}_{1-x}\text{Cu}_x\text{Ga}$. *Appl. Phys. Lett.* **88**, 192511 (2006).

- [10]. Ullakko, K., Huang, J. K., Kantner, C., O Handley, R. C. & Kokorin, V. V., Large magnetic-field-induced strains in Ni₂MnGa single crystals. *Appl. Phys. Lett.* **69**, 1966 (1996).
- [11]. Biswas, C., Rawat, R. & Barman, S. R., Large negative magnetoresistance in a ferromagnetic shape memory alloy: Ni_{2+x}Mn_{1-x}Ga. *Appl. Phys. Lett.* **86**, 202508 (2005).
- [12]. Khan, M., Dubenko, I., Stadler, S. & Ali, N., Magnetic and structural phase transitions in Heusler type alloys Ni₂MnGa_{1-x}In_x. *J. Phys.: Condens. Matter* **16**, 5259 (2004).
- [13]. Khan, M., Dubenko, I., Stadler, S. & Ali, N., The structural and magnetic properties of Ni₂Mn_{1-x}M_xGa (M=Co, Cu). *J. Appl. Phys.* **97**, 10M304 (2005).
- [14]. Gautam, B. R., Dubenko, I., Mabon, J. C., Stadler, S. & Ali, N., Effect of small changes in Mn concentration on phase transition temperatures and magnetic entropy variations in Ni₂Mn_{0.75}Cu_{0.25}Ga Heusler alloys. *J. Alloys and Comp.* 2008 (in press).
- [15]. Kübler, J., Williams, A. R. & Sommers, C. B., Formation and coupling of magnetic moments in Heusler Alloys. *Phys. Rev. B* **28**, 1745 (1983).
- [16]. Şaşıoğlu, E., Sandratskii, L. M. & Bruno, P., Role of conduction electrons in mediating exchange interactions in Mn-based Heusler alloys. *Phys. Rev. B* **77**, 064417 (2008).
- [17]. Bhoje, P. A., Priolkar, K. R. & Sarode, P. R., Local atomic structure of martensitic Ni_{2+x}Mn_{1-x}Ga: An EXAFS study. *Phys. Rev. B* **74**, 224425 (2006).
- [18]. Brown, P. J. *et al*, The crystal structure and phase transitions of the magnetic shape memory compound Ni₂MnGa. *J. Phys: Condens Matter* **14**, 10159 (2002).

- [19]. Ayuela, A., Enkovaara, J. & Nieminen, R. M., *Ab initio* study of tetragonal variants in Ni₂MnGa alloy. *J. Phys.: Condens. Matter* **14** 5325 (2002).
- [20]. Barman, S. R., Banik, S. & Chakrabarti, A., Structural and electronic properties of Ni₂MnGa. *Phys. Rev. B* **72**, 184410 (2005).
- [21]. Zayak, A. T., Entel, P., Rabe, K. M., Adeagbo, W. A. & Acet, M., Anomalous vibrational effects in nonmagnetic and magnetic Heusler alloys. *Phys. Rev. B* **72**, 054113 (2005).
- [22]. Jakob, G., Eichhorn, T., Kallmayer, M. & Elmers, H. J., Correlation of electronic structure and martensitic transition in epitaxial Ni₂MnGa films. *Phys. Rev. B* **76**, 174407 (2007).
- [23]. Kimura, A. *et al*, Magnetic circular dichroism in the soft-x-ray absorption spectra of Mn-based magnetic intermetallic compounds. *Phys. Rev. B* **56**, 6021 (1997).
- [24]. Kallmayer, M. *et al*, Magnetic properties of Co₂Mn_{1-x}Fe_xSi Heusler alloys. *J. Phys. D: Appl. Phys.* **39**, 786 (2006).
- [25]. Wang, W. H. *et al*, Magnetic properties and spin polarization of Co₂MnSi Heusler alloy thin films epitaxially grown on GaAs(001). *Phys. Rev. B* **71**, 144416 (2005).
- [26]. Chakrabarti, A., Biswas, C., Banik, S., Dhaka, R. S., Shukla, A. K. & Barman, S. R., Influence of Ni doping on the electronic structure of Ni₂MnGa. *Phys. Rev. B* **72**, 073103 (2005).
- [27]. Brown, P. J., Bargawi, A. Y. Crangle, J., Neumann, K-U. & Ziebeck, K. R. A., Direct observation of a band Jahn–Teller effect in the martensitic phase transition of Ni₂MnGa. *J. Phys: Condens. Matter* **11**, 4715 (1999).

- [28]. Imada, S., Yamasaki, A., Kanomata, T., Muro, T., Sekiyama, A. & Suga, S.,
Composition dependence of Ni magnetic moment in Ni–Mn-based Heusler-type
intermetallic compounds. *J. Mag Mag. Mat.* **310**, 1857 (2007).
- [29]. Haskel, D. *et al*, Role of Ge in Bridging Ferromagnetism in the Giant
Magnetocaloric $\text{Gd}_5(\text{Ge}_{1-x}\text{Si}_x)_4$ Alloys. *Phys. Rev. Lett.* **98**, 247205 (2007).

Figure Legends:

Fig. 1. (a) Magnetization versus temperature curves for Ni₂MnGa (red circle) and Ni₂Mn_{0.75}Cu_{0.25} (blue triangle) for both increasing and decreasing temperature. (b) Neutron diffraction tracking the cubic (002) Bragg peak as a function of temperature for Ni₂Mn_{0.75}Cu_{0.25} showing the coexistence of cubic and tetragonal phase during the magneto-structural phase transition. Vertical dashed lines are guide to the eyes to show the peak positions. In the cubic phase $a = 5.814 \text{ \AA}$

Fig. 2. XAS curves at the Ni (a), Mn (b), Cu (c) and Ga (d) for Ni₂Mn_{0.75}Cu_{0.25} at 80 K (red line) and 330 K (black line). The XMCD curves temperatures 80, 300 and 330 K are shown in Fig. 2 (e-h). The inset in Fig. 2(a) shows the Ni XAS around the peak marked B, while the arrow in the inset of Fig 2(b) shows the Mn XAS around the feature marked F. Green lines in Fig. 2(c,d) and 2(g,h) are guides to the eye show the absence (presence) of XMCD at the L₃ peak of Cu(Ga) respectively.

Fig. 3. XAS curves at the Ni (a) and Mn (b) for Ni₂MnGa (blue line) and Ni₂Mn_{0.75}Cu_{0.25} (red line) at 80 K. Inset in Fig 3(a) shows the Ni XAS peak around the peak marked B. The arrow indicates the bump discussed in the text.

Fig. 4. (a-c) XMCD curves curves for Ni, Mn and Ga for Ni₂MnGa (blue line) and Ni₂Mn_{0.75}Cu_{0.25}Ga (red line) at T = 80 K. The peaks marked A and B are explained in the

text. The arrow in Fig. 3(c) indicates increased XMCD for Ga at the L_3 edge for Ni_2MnGa and $\text{Ni}_2\text{Mn}_{0.75}\text{Cu}_{0.25}\text{Ga}$.

Figures:

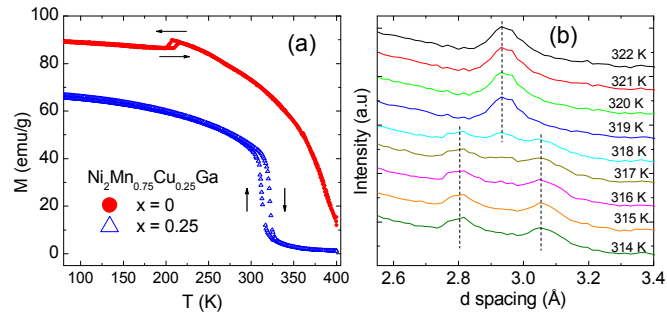


Fig. 1

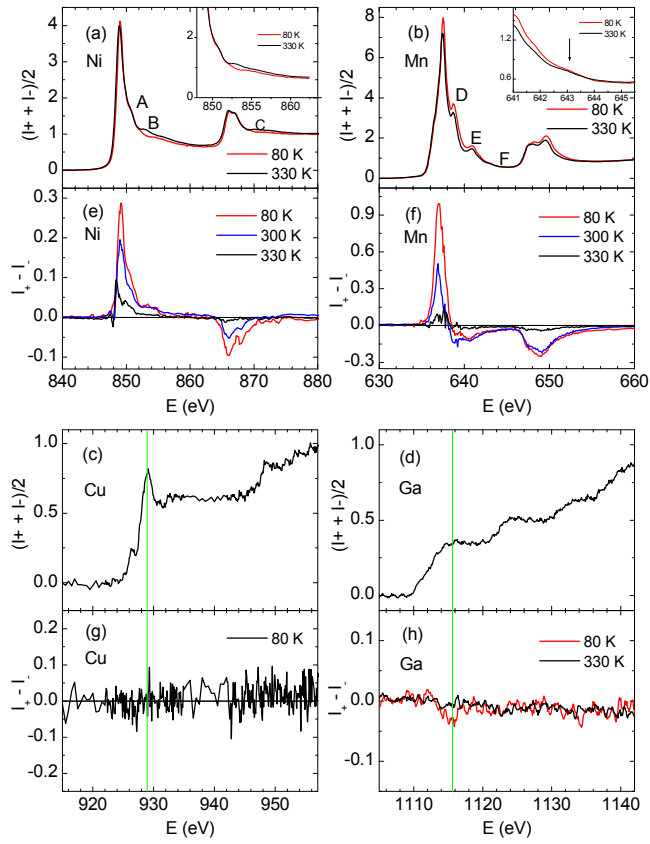


Fig. 2

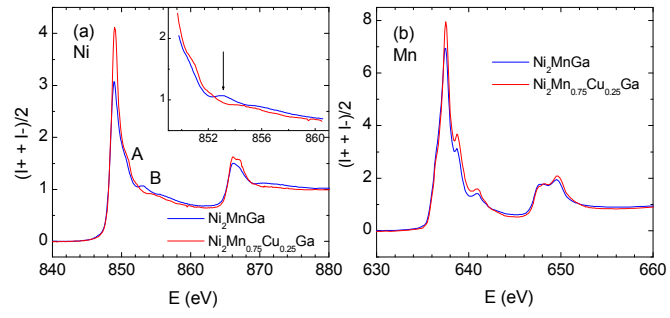


Fig. 3

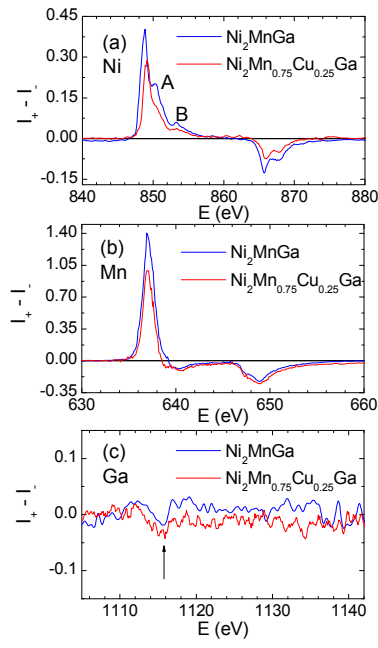


Fig. 4